ISSN: 3030-3346

APPROACHES TO EXTRACTING INFORMATIVE FEATURES FROM MRI IMAGES USING FILTERS: A METHODOLOGICAL STUDY OF PREPROCESSING FOR BREAST CANCER IMAGE ANALYSIS

Ungboyeva Mukaddas

Jizzakh branch of the National University of Uzbekistan named after Mirzo Ulugbek, Jizzakh, Uzbekistan
E-mail: mungboyeva@gmail.com

K E Y W O R D S

breast MRI; intensity normalization; CLAHE; Gaussian smoothing; Laplacian of Gaussian; radiomic features; preprocessing

A B S T R A C T

Reliable breast magnetic resonance imaging analysis begins with control of image intensity and spatial detail before features are extracted. This article examines two preprocessing methods, percentile based intensity normalization and contrast limited adaptive histogram equalization, together with two filter types, Gaussian smoothing and the Laplacian of Gaussian. Their roles are separated into intensity harmonization, local contrast redistribution, suppression of fine variation, and extraction of scale dependent structures. A reproducible two dimensional demonstration is performed on a publicly licensed published breast DCE-MRI image. Original, preprocessed, and filtered panels are presented alongside intensity distributions, line profiles, and filter sensitivity diagrams. Quantitative measurements describe changes in the displayed image rather than diagnostic performance. Gaussian filtering attenuates high frequency variation while LoG produces signed structural response maps that must be interpreted separately from anatomical grayscale images. The proposed workflow retains an unmodified reference and separates enhanced images from quantitative enhancement analysis. Its contribution is an auditable framework for the preliminary image processing stage of breast cancer detection. Clinical usefulness, lesion sensitivity, and early stage cancer discrimination require subsequent evaluation on volumetric MRI with pathology linked outcomes.

1 Introduction

Breast MRI provides complementary information about tissue morphology and contrast enhancement. Its relevance to selected screening populations is reflected in the recommendations of the European Society of Breast Imaging for women with extremely dense breasts [1]. Automated analysis nevertheless depends on the quality and consistency of the images supplied to a detector. A visible abnormality can be weakened by excessive smoothing, whereas local enhancement can make normal structures appear more prominent. The preprocessing stage therefore needs an explicit objective and a record of every transformation.

The phrase preliminary stage in this article refers to the first computational stage before lesion detection or classification. It does not mean that the demonstrated algorithm identifies a clinical cancer stage. The study concentrates on how image representations change and which feature families those representations can support. This distinction is necessary because an attractive filtered image alone cannot establish an improvement in cancer detection. MRI intensity values are sequence dependent and do not have the universal interpretation associated with a calibrated physical quantity. Receiver settings, field inhomogeneity, reconstruction, and acquisition protocol can all influence appearance. Within a breast examination, the relationship between precontrast and postcontrast intensity is also important. Applying an independent nonlinear contrast transformation to each temporal frame would alter that relationship. A suitable pipeline must distinguish the image used for visual feature generation from the image used to calculate enhancement kinetics.

Two practical questions guide the work. First, how can the available intensity range be made usable without treating the brightest isolated pixel as a reliable calibration point? Second, how

(cc) BY

can local variations be separated from spatial structures without removing potentially informative boundaries? Percentile normalization and CLAHE address the first question at different spatial levels. Gaussian and LoG filters address the second through low pass and derivative based representations, respectively.

The paper offers three concrete outputs: an explicit set of parameters for a display image experiment, a comparison between original and transformed images, and a validation design for transferring the approach to volumetric breast MRI. The methods are established techniques. The contribution is their transparent organization into a preliminary breast image analysis workflow, with measured image changes and clearly stated limits rather than a claim of a new diagnostic algorithm.

2 Related work

The Image Biomarker Standardisation Initiative provides an important framework for defining feature calculations and image processing settings. Its convolutional filter work emphasizes that kernel definitions and implementation details affect reproducibility [2]. This motivates the reporting of spatial scale, boundary handling, response polarity, and discretization in the present experiment. Reproducibility is a prerequisite for deciding whether an observed image feature is useful across examinations. Bias field correction is another relevant MRI preparation technique. N4ITK is a widely used approach to correcting slowly varying intensity nonuniformity [3]. It is discussed here as a prerequisite to consider in a volumetric study, not counted as one of the two implemented preprocessing methods. A cropped published JPEG cannot support a reliable estimate of the original acquisition bias field. Applying correction to that image and presenting it as scanner harmonization would exceed the information contained in the source.

CLAHE was developed to redistribute local grayscale values while limiting histogram amplification [4]. Unlike global normalization, it can change the contrast between nearby structures differently in different regions. Its value for a feature extraction branch must be balanced against amplification of noise and modification of tissue intensity relationships. Consequently, the original image is retained for comparison and clinical reading.

Gaussian smoothing and LoG filtering provide complementary representations. Gaussian smoothing averages nearby values with distance dependent weights; LoG measures second spatial derivatives after smoothing. The latter produces positive and negative responses rather than a denoised anatomical image. These responses can describe blobs and boundaries at selected scales, but their biological significance cannot be inferred solely from their magnitude.

3 Source and Study Design

The demonstration uses the public image Breast dce-mri.jpg, attributed to Zhen Lu Yang and licensed under Creative Commons Attribution 4.0 [5]. Its source is a panel from the study by Yang et al. [6]. The published case describes right breast ductal carcinoma in situ. That source description is used only to establish the context of the example; no independent diagnostic interpretation is made in this work. The downloaded source is a 378 by 297 pixel JPEG. It is a rendered publication image, not an original DICOM acquisition. It contains a modality label, a panel letter, and an arrow. To reduce interference from outer labels, the processing crop uses rows 45 through 284 and columns 10 through 366 in zero based indexing, producing 240 by 357 pixels. The resulting source crop is the reference for all computed panels. The original panel remains visible in Figure 1.

(cc) BY

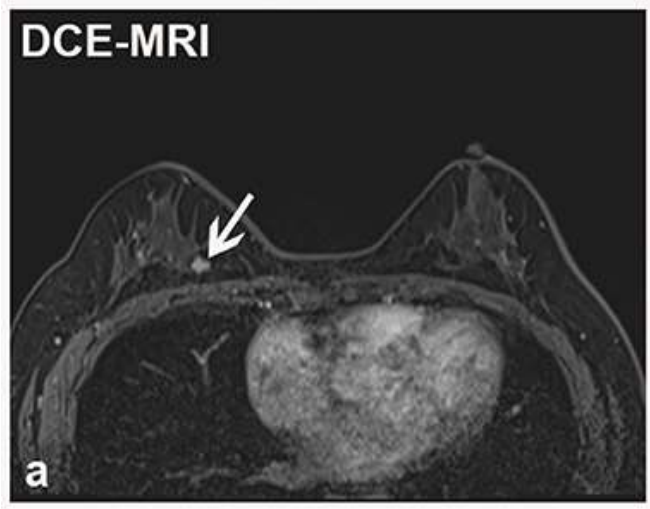


Figure 1. *Published breast DCE-MRI source panel. Credit: Zhen Lu Yang, via Wikimedia Commons [5], from Yang et al. [6], CC BY 4.0. The arrow and labels belong to the source image.*

All transformations operate on the same grayscale crop converted to floating point values in the interval from zero to one. A descriptive foreground proxy is defined by source intensity greater than 0.12. The rectangle at crop rows 55–114 and columns 95–139 is excluded from that proxy to reduce the influence of the published arrow. This proxy is an intensity sampling region; it is neither a breast segmentation nor a tumor mask. No lesion specific contrast or diagnostic metric is calculated. The experimental unit is one display image. Pixels are spatially dependent samples within that image and are not independent patients. No significance test, clinical confidence interval, or classifier accuracy is reported. This design supports implementation and illustration of image transformations, while preventing a single published example from being misrepresented as a clinical cohort.

4 Two preprocessing methods

4.1 Percentile based intensity normalization

The first method estimates lower and upper reference intensities from the foreground proxy. The 1st and 99th percentiles are used to reduce sensitivity to extreme values. Intensities below the lower reference are clipped to zero, intensities above the upper reference are clipped to one, and the remaining values are linearly rescaled. Equation (1) defines the transformation, where I is the grayscale crop and q denotes a percentile calculated within the sampling region.

$$N(x) = clip((I(x) - q_1) / (q_{99} - q_1), 0, 1) \quad (1)$$

For this image, the calculated reference values are $q_1 = 0.121569$ and $q_{99} = 0.623529$ in relative grayscale units. If the two references coincide, the image should be flagged as degenerate rather than divided by an arbitrarily small number. The transformation preserves intensity order inside the unclipped interval, but clipping can eliminate distinctions in its tails. A study interested in very bright enhancing tissue should inspect which voxels are clipped before accepting these percentiles.

The method changes scale and offset; it does not remove noise, correct geometric distortion, or estimate a physical tissue property. Foreground selection is critical: including a large dark background would shift the percentile estimates. For volumetric breast MRI, the sampling region should be anatomically defined and consistent across examinations. If a learned reference is used, its parameters must be estimated within training data only.

4.2 Contrast limited adaptive histogram equalization

The second method divides N into an 8 by 8 grid and estimates a 256 bin histogram in every tile. A clipping threshold limits large histogram counts. The clipped excess is redistributed uniformly across all bins, and each resulting cumulative histogram defines a local intensity mapping. Bilinear interpolation between tile mappings reduces discontinuities. The experiment uses a count threshold of max(1, 2n/256), where n is the number of pixels in the tile.

$$C(x) = Tlocal(N(x)) \quad (2)$$

The clip multiplier of two is an implementation specific parameter, not a universal MRI optimum. It should not be equated with a

similarly named parameter in another software library without comparing the definitions. A fixed grid, defined clipping rule, and stated interpolation method are therefore part of the reproducibility record. At the outer tile centers, interpolation coordinates are clamped to the nearest available center.

CLAHE redistributes contrast in weakly varying regions and may make boundaries easier to examine. It can also increase the visibility of reconstruction texture and background variation. In the proposed workflow, C is an auxiliary feature image. Enhancement curves, apparent diffusion coefficient values, and quantitative sequence measurements remain on appropriate original or physically calibrated data, because a local nonlinear mapping would change their interpretation.

5 Two filter types and their expected effects

5.1 Gaussian smoothing

Gaussian filtering produces a weighted local average. For a continuous two dimensional model, Equation (3) gives the kernel, with spatial standard deviation σ. The filtered intensity representation is obtained by convolving the selected input with this kernel. In the experiment, Gaussian filtering is applied directly to the CLAHE image C, with σ = 1 pixel and a support truncated at four standard deviations.

$$G\sigma(u,v) = exp(-(u^2 + v^2)/(2\sigma^2)) / (2\pi\sigma^2) \quad (3)$$

$$S\sigma = G\sigma * C \quad (4)$$

The discrete kernel is normalized by the implementation so that a constant input remains constant. Reflective boundary handling is used at the crop margins. Gaussian smoothing attenuates fine fluctuations and JPEG texture, but the same operation attenuates fine anatomical detail. A narrow spicule or a small focus can become less distinct as σ increases. The appropriate strength must therefore be determined using annotated lesion data rather than global smoothness alone.

5.2 Laplacian of Gaussian

LoG combines smoothing with the Laplacian, the sum of second derivatives along the image axes. Equation (5) specifies the sign convention and scale normalization used here. The response is calculated directly from C rather than from Sσ, avoiding an additional unreported smoothing stage. The main illustration uses σ = 2 pixels, while a separate comparison uses one, two, and three pixels.

$$R\sigma = -\sigma^2 [\partial^2(G\sigma * C)/\partial u^2 + \partial^2(G\sigma * C)/\partial v^2] \quad (5)$$

A bright structure can produce a positive center response under this sign convention and negative surrounding responses. Magnitudes depend on scale, local contrast, and structure size. Positive and negative responses are retained for numerical feature extraction. A diverging colormap is used only for visualization, with a symmetric limit determined from the 99th percentile of absolute response. The display limit does not clip the stored floating point response used in calculations.

Figure 2 shows the workflow and the conceptual separation between intensity features and structural response features. For the illustrated experiment both filters are applied to C; the diagram also highlights that a future quantitative branch can use normalized intensities without CLAHE. Filter outputs are complementary representations and should not be interpreted as two competing diagnostic decisions.

(cc) BY

ISSN: 3030-3346

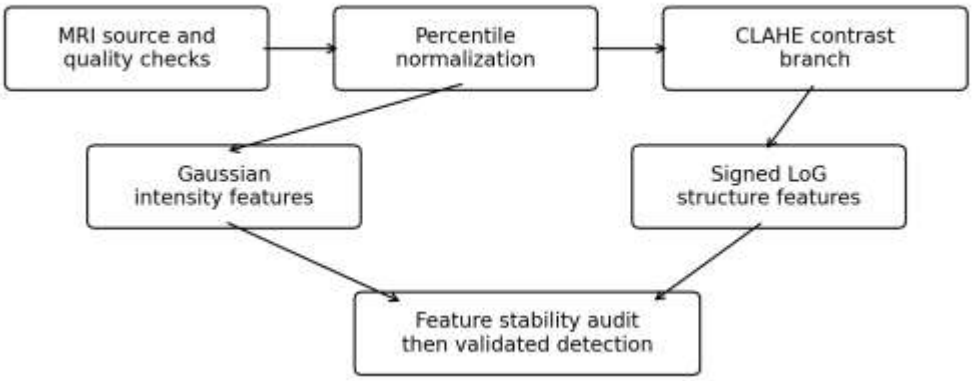


Figure 2. *Proposed preprocessing and feature analysis workflow. Enhanced and quantitative branches require separate validation.*

6 Features and Evaluation Measures

Feature informativeness has two distinct meanings. An image descriptor may change substantially after filtering, yet that change may carry no information about malignancy. This study measures the former. The latter requires association with independent labels and validation outside the data used to select processing parameters. Figure 3 presents the original crop, the two preprocessing outputs, the Gaussian image, the signed LoG map, and a residual image.

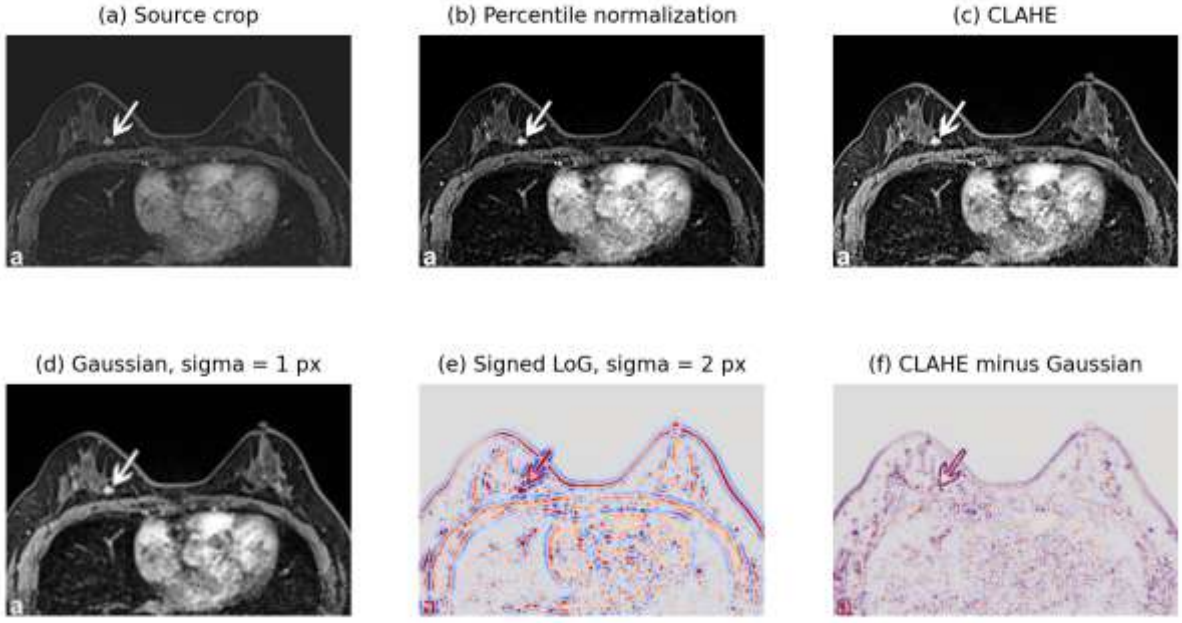


Figure 3. *Original source crop and computed transformations. Panels (a–d) use a common 0–1 grayscale display. Panels (e–f) use separate symmetric response ranges. Adapted from [5], CC BY 4.0; cropping and transformations were performed for this study.*

First order descriptors include mean, standard deviation, and histogram entropy within the fixed sampling region. Entropy is calculated with 64 equal width bins over zero to one. The same region and bin edges are used for source, normalized, CLAHE, and Gaussian images. This makes the reported numbers comparable as display

(cc) BY

image descriptors, but does not make them tumor biomarkers.

$$H = -\Sigma\, p_{\mathrm{i}}\, log_2(p_{\mathrm{i}}) \quad (6)$$

Spatial variation is summarized using mean gradient energy. The horizontal and vertical gradients are estimated by Sobel derivatives divided by eight, and the squared components are added before averaging. This normalization convention is included because the numerical magnitude depends on the derivative operator. Gradient energy can decrease when noise is reduced, when a boundary is blurred, or both; it does not identify which effect occurred.

$$E\nabla = mean[(D_{\mathrm{u}}I)^2 + (D_{\mathrm{v}}I)^2] \quad (7)$$

Potential downstream descriptors include intensity dispersion on normalized images, texture statistics after fixed discretization, and signed response statistics at each LoG scale. Shape descriptors require a real lesion mask and should be extracted from its geometry. In particular, a thresholded LoG response must not be reported as a validated tumor contour. Texture calculations also need a stated voxel spacing and neighborhood definition, which this JPEG source cannot provide.

7. Results of the display image experiment

Table 1 reports measurements computed on the fixed foreground proxy. The values describe this one cropped display image. Changes in entropy or gradient energy summarize redistribution and smoothing; their direction is not interpreted as evidence of improved cancer discrimination.

Table 1.

Measured descriptors within the fixed sampling region

Representation	Mean	SD	Entropy bits	Gradient energy
Source crop	0.2401	0.1319	4.4535	0.001638
Normalized	0.2344	0.2558	5.1341	0.005479
CLAHE	0.2862	0.2599	5.4432	0.009068
Gaussian	0.2839	0.2436	5.4354	0.003568

The source and normalized images retain the same spatial arrangement. The normalization changes dynamic range and clips tail intensities, so their mean and dispersion need not agree. CLAHE changes the mapping locally, widening some weak variations and compressing others. The Gaussian representation reduces rapid spatial variation in its CLAHE input. The residual in Figure 3f locates the detail removed by this smoothing, including both anatomy related variation and image artifacts.

Figure 4 provides two additional views of the same transformations. The histogram is calculated within the sampling region. The line profile uses fixed crop row 145 across the full image width and is intended only to show spatial smoothing. It is not a line placed through an independently annotated tumor and must not be interpreted as a lesion boundary measurement.

(cc) BY

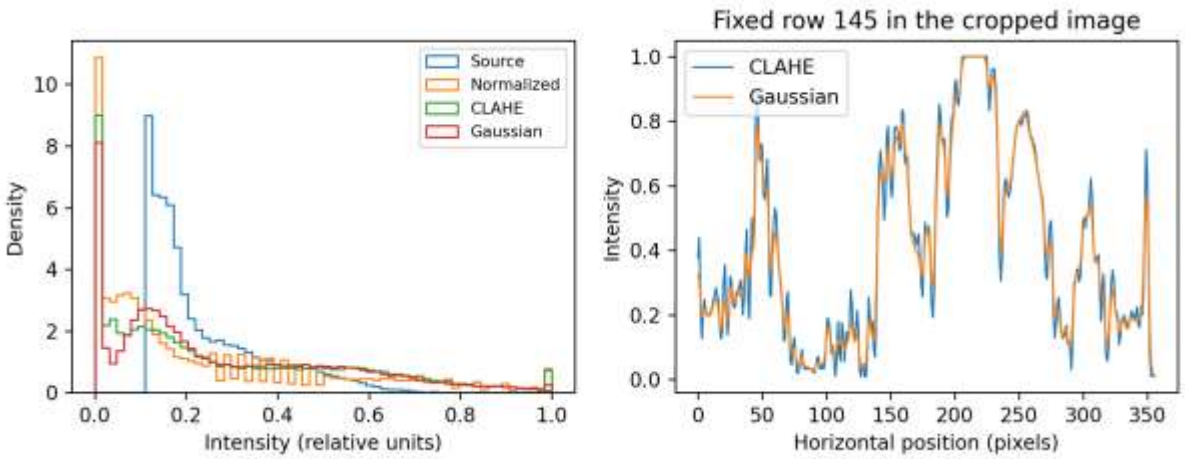


Figure 4. *Intensity distributions and fixed horizontal line profiles. Values refer to the cropped JPEG experiment, not calibrated MRI signals.*

A smoother line profile can be beneficial for a feature dominated by high frequency artifacts, yet detrimental for a feature that depends on a narrow edge. This explains why no single global descriptor is used as the optimization target. The visual and numeric results together establish that the implementation produces different representations; they do not establish which representation a detector should prefer.

LoG is excluded from the grayscale mean and entropy comparison because its signed response domain has a different meaning and scale. Converting it to a zero to one display and comparing the resulting entropy with anatomical intensity would mix a visualization choice with the image analysis result. A proper LoG feature table would report response statistics with the sign convention and scale attached to every descriptor.

8. Parameter sensitivity and interpretation

Gaussian strength was varied over $\sigma = 0.5$, 1, 1.5, 2, and 3 pixels. Figure 5 reports full crop gradient energy and root mean squared difference from the CLAHE input. Unlike Table 1, these sensitivity calculations cover the entire crop; their values should therefore not be substituted for the masked gradient energy values. The input C is a comparison reference, not a noise free ground truth.

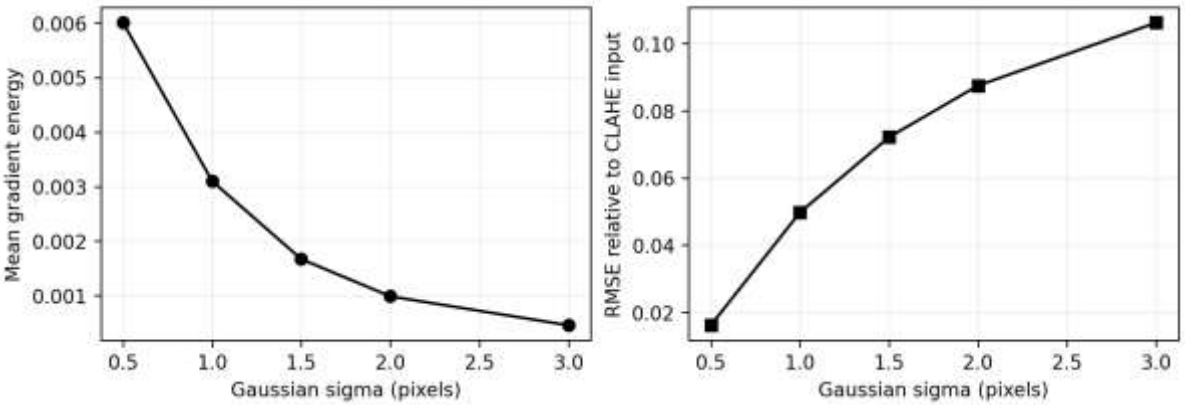


Figure 5. *Gaussian parameter sensitivity on the full crop. RMSE measures transformation magnitude relative to C; it is not a denoising accuracy measure.*

(cc) BY *dtai.uz*

ISSN: 3030-3346

Increasing the spatial averaging scale removes progressively broader variation and increases the departure from the input. This is an expected mathematical effect of low pass filtering. It does not demonstrate that larger σ is preferable. Small lesions and thin boundaries are exactly the structures that can be suppressed when the scale is enlarged. Parameters expressed in pixels cannot be transferred directly to another acquisition with a different voxel spacing. Figure 6 illustrates the scale dependent LoG responses. Each panel uses its own symmetric display limit for readability. Consequently, response brightness cannot be compared quantitatively across the panels. The change in spatial extent is informative: larger scales respond to broader structures, while smaller scales retain finer detail. A future clinical study should express scales in millimeters and account for anisotropic sampling.

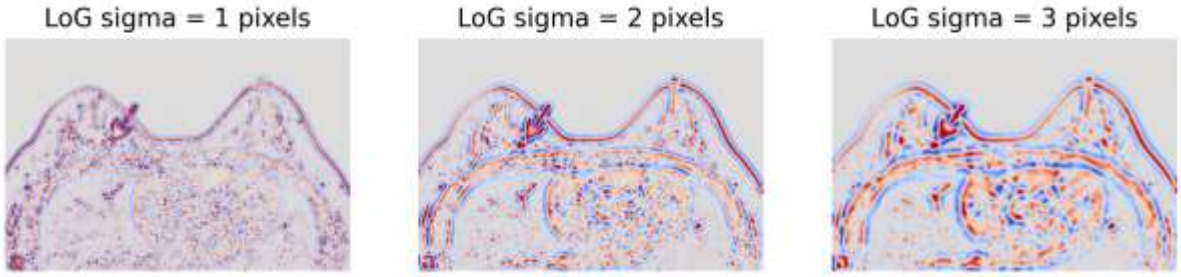


Figure 6. *Signed LoG responses at three scales. Independent display ranges are used; cross scale intensity comparisons require the stored numerical responses.*

The published annotation arrow remains visible in the crop and may produce strong derivative responses. Its exclusion from the descriptive sampling region reduces one source of bias but does not remove it from the filtered panels. This is a further reason to limit the interpretation to an implementation demonstration and to use unannotated DICOM or NIfTI images for subsequent modeling.

A clinical extension should begin with complete, deidentified MRI volumes and documented sequence metadata. One possible research resource is the Duke Breast Cancer MRI collection hosted by The Cancer Imaging Archive [7]. A cancer cohort alone is insufficient for validating a screening detector: benign findings and appropriately followed negative examinations are also needed. Patient outcomes, lesion locations, and the intended diagnostic task must be defined before parameter selection.

The minimum ablation compares normalized images alone, normalized plus CLAHE, normalized plus Gaussian, normalized plus LoG, and a combined feature set. Identical patient partitions and classifier settings should be used across these conditions. All slices from one patient must remain in a single partition. Feature scaling, feature selection, and any data driven normalization are fitted using training data only. An external institution should be reserved for evaluating scanner and protocol transfer.

For candidate detection, the relevant outcomes include lesion sensitivity at a stated false positive rate per examination, performance by lesion size, and agreement with radiologist marked locations. For benign versus malignant classification, ROC-AUC, sensitivity, specificity, calibration, and confidence intervals can be reported on an independent test cohort. A claim concerning early stage disease additionally requires stage labels and sufficient representation of those cases. No such claim follows from the present demonstration.

(cc) BY

Table 2.

Validation questions for the next research stage

Question	Required evidence
Are small findings retained?	Annotated lesions, size stratification, blinded review
Are features repeatable?	Repeat scans or controlled image perturbations
Does filtering improve prediction?	Matched ablation on independent patient outcomes
Does the workflow transfer?	External scanners, institutions, and protocols

The limitations are substantial and specific. The experiment contains one compressed, annotated publication image; original acquisition intensities, voxel geometry, temporal phases, and a lesion mask are unavailable. Normalization and local contrast enhancement operate on rendered grayscale values. No new patients were enrolled, no cancer detector was trained, and no pathology linked performance was estimated. These constraints do not invalidate the observed transformations, but they restrict the work to a methodological preliminary study.

9 Conclusion

Percentile normalization and CLAHE provide global and local intensity preparation, respectively. Gaussian filtering produces a smoother intensity representation, while signed LoG responses expose structures at chosen spatial scales. The original and transformed panels, descriptive measurements, and parameter diagrams make those effects inspectable. The workflow is suitable as a documented starting point for breast MRI feature extraction, provided that the reference image is retained and enhanced representations are separated from quantitative sequence analysis. Its clinical value must be established through lesion preserving parameter selection and independent patient level validation.

References

1. R. M. Mann et al., “Breast cancer screening in women with extremely dense breasts recommendations of the European Society of Breast Imaging (EUSOBI),” European Radiology, vol. 32, no. 6, pp. 4036–4045, 2022. doi: 10.1007/s00330-022-08617-6. https://doi.org/10.1007/s00330-022-08617-6
2. P. Whybra et al., “The Image Biomarker Standardization Initiative: Standardized Convolutional Filters for Reproducible Radiomics and Enhanced Clinical Insights,” Radiology, vol. 310, no. 2, article e231319, 2024. doi: 10.1148/radiol.231319. https://doi.org/10.1148/radiol.231319
3. N. J. Tustison et al., “N4ITK: Improved N3 Bias Correction,” IEEE Transactions on Medical Imaging, vol. 29, no. 6, pp. 1310–1320, 2010. doi: 10.1109/TMI.2010.2046908. https://doi.org/10.1109/TMI.2010.2046908
4. K. Zuiderveld, “Contrast Limited Adaptive Histogram Equalization,” in Graphics Gems IV, P. S. Heckbert, Ed. Academic Press, 1994, pp. 474–485. https://www.cse.unr.edu/~bebis/CS474/StudentPaperPresentations/1994%20-%20CLAHE.pdf
5. Z. L. Yang, “Breast dce-mri.jpg,” Wikimedia Commons, 2021. Image, 378 × 297 pixels, CC BY 4.0. Accessed Oct. 3, 2026. https://commons.wikimedia.org/wiki/File:Breast_dce-mri.jpg
6. Z. L. Yang et al., “Detection and Classification of Breast Lesions With Readout-Segmented Diffusion-Weighted Imaging in a Large Chinese Cohort,” Frontiers in Oncology, vol. 11, article 636471, 2021. doi: 10.3389/fonc.2021.636471. https://doi.org/10.3389/fonc.2021.636471
7. The Cancer Imaging Archive, “Duke-Breast-Cancer-MRI,” dataset collection. Accessed Oct. 3, 2026. https://www.cancerimagingarchive.net/collection/duke-breast-cancer-mri/

(cc) BY